IAC-24-D1.4.1,x84017

TETHER MANAGEMENT AND DOCKING SYSTEM FOR MULTI-ROBOT RAPPELLING INTO LUNAR LAVA TUBES

Jonathan Babel[a]*, Leon Cedric Danter[a], Gonzalo Paz Delgado[b], Raúl Dominguez[a], Yogeshkarna Govindaraj[a], Mehmed Yüksel[a] and Frank Kirchner[c]

[a] *DFKI Robotics Innovation Center, Robert-Hooke-Str. 1, 28359 Bremen, Germany,*
[b] *Space Robotics Laboratory, Department of Systems Engineering and Automation, Universidad de Málaga, Andalucia Tech, 29070 Málaga, Spain*
[c] *Robotics Research Group, University of Bremen, Bibliothekstraße 1, 28359 Bremen, Germany*
* Corresponding Author: *jonathan.babel@dfki.de*

Subsurface lava tubes have been detected from orbit on both the Moon and Mars. These natural voids are potentially the best place for long-term human habitations, because they offer shelter against radiation and meteorites. Skylights, formed by partial cave ceiling collapse, provide an entrance to several of the previously discovered lava tubes. Multi-robot collaboration may allow us to reach and explore these unknown cavities, where sending astronauts without prior knowledge is an evitable risk. This work presents the development and implementation of a novel Tether Management and Docking System (TMDS) designed to support the vertical rappel of a rover through a skylight into a lunar lava tube. The TMDS connects two rovers via a tether, enabling them to cooperate and communicate during such an operation. Its hardware comprises an active winch and two interfaces, a passive HOTDOCK and a passive EMI. Although particular robotic systems are used to demonstrate the feasibility of the task, the device can link any robots equipped with the active counterparts of these standard interfaces. The height of the TMDS platform can be adjusted by two linear actuators in order to facilitate docking and transport. A robotic software framework independent interface provides control over the platform height and the velocity at which the winch releases the tether. The winch speed is synchronized with the wheel speed of the rappelling rover allowing for a controlled descent. The development of hardware and software components is part of the Cooperative Robots for Extreme Environments project. In January and February 2023, the approach was thoroughly tested in a three-week lunar analogue mission on Lanzarote, Canary Islands. As a result, the collaborative multi-robot rappel into a lava tube was successfully showcased within the field tests.

Keywords: Tether Management System, Rappelling, Lava Tube, Skylight, Planetary Exploration, Space Robotics

1. Introduction

The European Commission launched the Horizon 2020 Strategic Research Cluster (SRC) in Space Robotics to foster European competitiveness of global space systems. Within the SRC a total of fourteen research projects [1–14] have been funded through Operational Grants (OG). Starting in 2016, the aim of the first projects was to develop robotic building blocks (OG1-OG6), and in the second phase, from 2019 onward (OG7-OG11), to integrate them towards orbital and planetary missions. The last phase from 2021 to 2023 was engaged to mature the mission of demonstration (OG12-OG14). Being the final Horizon 2020 project, the Cooperative Robots for Extreme Environments (CoRob-X) project is based on the heritage of the previous SRC building blocks.

A challenging mission scenario was chosen to validate the maturity of existing robotic space technologies and to assess their usability for terrestrial applications. More specifically, CoRob-X showcased how hard-to-reach areas on planetary surfaces, such as lava tubes on the moon and mining tunnels on Earth, can be explored with teams of cooperating autonomous robots.

Orbital photographic and remote sensing surveys of the Moon and Mars have shown evidence of lava tube formation [15]. These caverns form as the result of lava flows that have overcrusted to form subsurface flowing rivers of lava, as they drain an open conduit is left behind. Oberbeck et al. [16] describes such a lava tube on the Moon within the Northern Oceanus Procellarum region. It is approximately 40 km in length, based on imagery from Lunar Orbiter 5, Frame 182. Moreover, skylight entrances to lava tubes, formed by the partial collapse of the lava tube ceiling, have been noted on Mars in THEMIS imagery [17].

Lava tubes and cavities are of high scientific interest, as they represent a prime location to focus the search for life and water ice. To the geologist, lava tubes are useful in understanding the history of volcanism as well as the thermal flow on those celestial bodies. In addition, space agencies have considered to build permanent human habitats on the Moon and Mars. Lava tubes feature characteristics that would be beneficial to the establishment of such an in-situ science laboratory [18]. Caves provide protection from solar particle event (SPE) radiation and temperature changes are milder than on the surface. Those natural voids could serve as shelter in future astronaut missions, as they could be used to store materials and detain regolith dust [19]. The implications for logistical and mission planners are that a substantially larger fraction of the landed mass can be dedicated to life support and science mission support. This could enable longer duration missions without risk of radiation overdosing, better reliability and a more diverse set of scientific technology, and a larger habitat
area in which to work [15]. Thus, lava tubes are targets for planetary exploration missions. The open question is which caves on the Moon and Mars are suitable for human habitats, as images from orbiters only provide pictures of the entry.

This work presents an innovative Tether Management and Docking System (TMDS) used to explore planetary lava tubes with a multi-agent robotic team. Emphasis is put on the novel hardware design and software modules required to carry out the elaborate rappelling operation. Finally, the performance of the TMDS is evaluated in extensive field tests and suggestions for design improvements are derived.

The paper is organized as follows: (1) an introduction is given to the European SRC in Space Robotics and the scientific interest in lunar and Martian lava tubes; (2) describes the lunar analogue mission of the CoRob-X project and in particular the rappelling scenario; (3) presents previous work on TMDS, before focusing on (4) the implemented hardware and software; (5) comprises the final experimental validation; (6) concludes on the outcomes and provides an outlook to future research aspirations.

2. Mission Overview

The CoRob-X project covers two large-scale field tests. A Lunar Analogue Mission at the La Corona Lava Tube System on Lanzarote, Canary Islands and a Terrestrial Demonstrator in a mining tunnel of the Fundación Santa Bárbara, located in León, Spain. A project introduction is given by [13] and the overall results are summarized by [14]. Dominguez et al. [20] provide further insight in the selection of the analogue site. The multi-robot

Fig. 1. The multi-robot team: SherpaTT (left), Coyote3 (mid) and LUVMI-X (right)

rappelling with the TMDS is part of the Lunar Analogue Mission. Hence, in the following a short mission overview is given and the rappelling scenario is described in more detail.

The Lunar Analogue Mission demonstrates the exploration of a lava tube through a skylight with a heterogeneous robotic team, depicted in Figure 1. The field test is divided into four Mission Phases (MP1-4) as shown in Figure 2. At first, the three rovers SherpaTT [21], Coyote3 [22] and LUVMI-X [23] collaboratively explore and map the area around the skylight (MP-1). During the exploration, SherpaTT carries an avionics box, developed by project partner GMV, that provides the required processing power and sensors to perform Guidance, Navigation and Control (GNC). It uses the LocCams and Inertial Measurement Unit (IMU) from the avionics box to obtain localization with visual odometry, and the NavCams to create a detailed map of the environment. Coyote3 is equipped with a prototype of the Ground Penetrating Radar (GPR) designed for the Rosalind Franklin rover [25] for the ExoMars mission of the European Space Agency (ESA). The WISDOM [24] GPR records cross-sectional radar grams of the subsurface to estimate the extent of the lava tube system. In the next phase (MP-2), LUVMI-X ejects a sensor cube through the skylight into the lava tube to gather information about rock formations along the vertical walls and from the landing site, allowing to identify the best entry point for the rappelling. In the third phase (MP-3), Coyote3 rappels down into the skylight, assisted by movements of SherpaTT's manipulator to maintain a constant tension on the tether. Once Coyote3 has reached the ground, it undocks from the TMDS and explores the lava tube system (MP-4).

In Mission Phase 3, the following software modules are of key importance: *TMDS Deployment*, *Docking Behaviour*, *Rappelling Guidance* and *Mobile Manipulation*. SherpaTT uses its 6 DoF manipulator to grasp the TMDS, which initially is attached to the body, and lowers it to the ground in the vicinity of the skylight. The software module TMDS Deployment synchronizes manipulator and wheel motions of the rover with the unwinding speed of the tether to ensure a smooth deployment in uneven terrain. After the TMDS has been placed on the ground, the Docking Behaviour module orchestrates the docking of Coyote3 with the TMDS. Once a rigid connection between Coyote3 and the TMDS has been established, Rappelling Guidance controls the tethered descent of Coyote3 into the lava tube. Meanwhile, the Mobile Manipulation module protects the manipulator of SherpaTT from high torques during the rappelling operation.

3. Related Work

Tether Management Systems (TMS) have raised research interest in space robotics since they provide the means to enhance the mobility of planetary rovers. A survey on tether concepts and previous tether missions

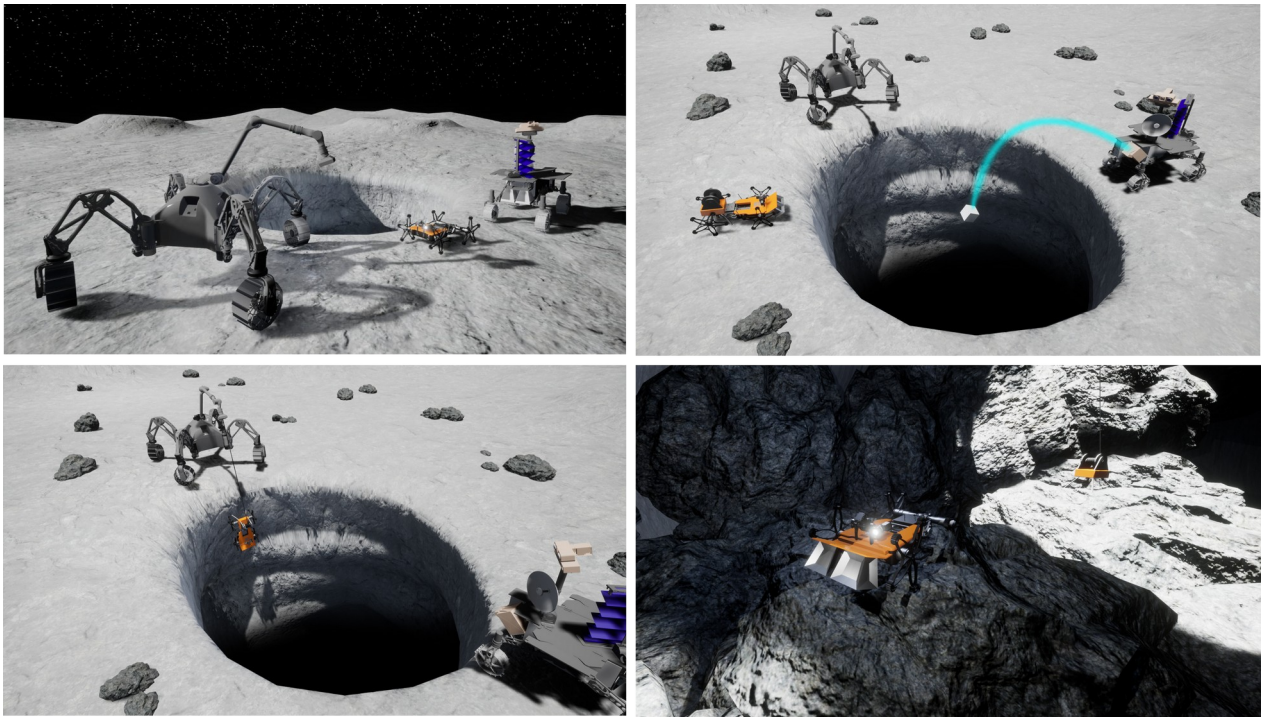

Fig. 2. The four phases of the CoRob-X Lunar Analogue Mission: MP-1 (top left) - collaborative mapping of the area around the skylight, MP-2 (top right) - sensor cube injection into the skylight, MP-3 (bottom left) - rappelling of Coyote3 to the bottom of the lava tube, and MP-4 (bottom right) - subsurface lave tube exploration.

in space is given by [26]. One of the most impressive examples of tether usage is the Sky Crane Maneuver [27]. The maneuver is the last part of the entry, descent and landing phase for the two rovers, Curiosity and Perseverance, set on Mars by NASA in 2021. Several Tethered Rovers (TRs) have been developed and tested in the past. Dante I and II [28] were the first tethered climbing systems to be designed and deployed in extreme terrain. TRESSA [29] is an advanced concept involving three robots to explore steep areas. In this concept, two robots act as anchors for the third, which is suspended on tethers to perform lateral movements on a steep or near vertical wall. A more simplistic tethering concept is Axel [32], developed by the Jet Propulsion Laboratory. Its two-wheel design allows it to continue operating even in the event it flips over and the boom provides a conduit for the tether to avoid entanglement. DuAxel [32] is a redundant four-wheeled platform using two Axel robots. Another approach for accessing and maneuvering on steep terrain is TReX [30, 31]. Its main feature is a rotating tether arm that enables the skid-steered rover body to move laterally to the tether on steep slopes. The arm guiding the tether is angled downward so that the tether is in line with the rover's center of mass, while the spool rests on top of the rover platform. This prohibits the introduction of forces that would tilt the chassis in the direction of the tether. Additionally, highly mobile non-tethered robots for lunar crater exploration and steep terrain exist. Examples of such concepts are the six-legged robot SpaceClimber [33] and the hybrid legged-wheel rover Coyote3 [22].

Apart from the TMS and the design of the tethered robot, attention must be paid to the requirements of the tether itself. The tether provides mechanical support, power and communication from a surface rover, which serves as an anchoring point, to a highly mobile rover foreseen to rappel down into the lava tube. Several tether prototypes have been developed and characterized for their mechanical, electrical, and environmental properties [34]. Nesnas et al. [35] summarizes the results of testing a specific tether, characterizing its static and dynamic load capability, bending and abrasion resistance.

Our proposed design allows both robots involved in the rappelling operation to dock and undock from the TMDS. Therefore, suitable interfaces for the connection between the TMDS and the robots must be selected. A comprehensive review of such interfaces is given by [36] and a new standard interface for space robotics is described in [37]. Within the CoRob-X project, two consortium partners provide their own interface solutions: on the one hand, the Electro-Mechnical Interface (EMI) [38] from *German Research Center of Artificial Intelligence* and, on the other hand, the HOTDOCK [39] from *Space Application Services*.

The motivation for our novel TMDS design is meant to address limitations of all prior systems. Because the TMDS is designed as a standalone platform with standard space robotic interfaces, conceivably any planetary rover equipped with these interfaces can be part of a multi-robot rappelling mission. With our approach, the development of mobile robots for extreme terrain can be decoupled from engineering the TMS to the greatest extent. Another benefit of our approach is the extended exploration range, as the scout rover is able to undock from the TMDS, it can advance further into the subsurface lava tube system and subsurface exploration without being attached to the tether reduces the risk for entanglement.

4. Hardware and Software Developments

4.1 Tether Management and Docking System

4.1.1 Hardware

The structure of the TMDS is composed of a lightweight aluminum frame and carbon fiber sheets, depicted in Figure 3. Its total weight, including the on-board tether, is 23 kg. The tether has a length of 30 m and an off-the-shelf submarine cable is used as the improvement of existing tethers for space applications [34] is not within the scope of this work. The tether is reeled off an active winch and tensioned by a pulley mechanism that employs a force sensor to monitor the tether's tension and prevent slack. The built-in force

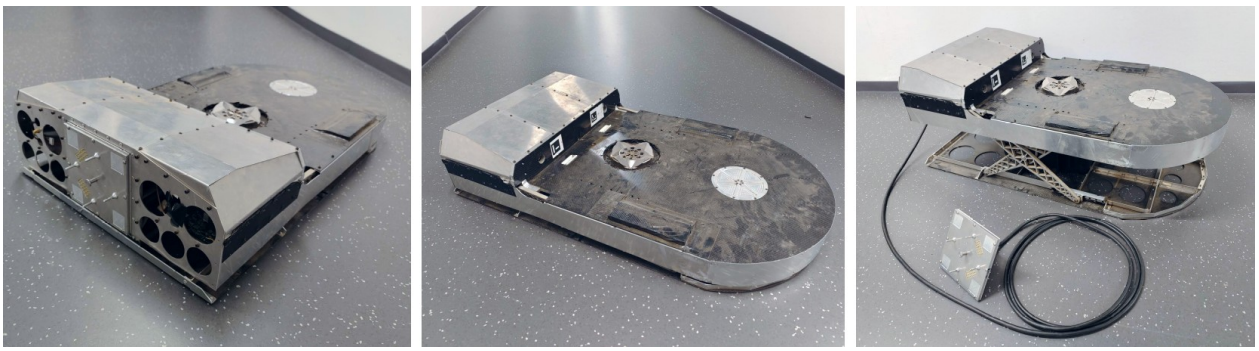

Fig. 3. TMDS rear (left) and front view (centre) folded as well as in extended state (right) with partially uncoiled tether.

sensor is a tension compression load cell with a measuring range of ±2 kN and an accuracy error of max. ±0.25% F.S. Table 1 summarizes the technical specifications of the developed hardware.

Table 1. TMDS Technical Specifications

Category	Value	Category	Value
Dimensions	920 mm length, 520 mm width	Tether	30 m
	87 mm height (folded)	Force Sensor	Burster 8435-6002
	300 mm height (extended)	Interfaces	EMI, HOTDOCK
Mass	23 kg (including tether)	Connectivity	OM2P mobile access point,
Actuators	1x Robodrive ILM 70x18		Netgear GS305E switch
	2x Robodrive ILM 38x12	Structure	Lightweight aluminum
Transmission	1x HD CSD 32-2A-160		frame & carbon fibre sheets
	2x ball screw spindle	Voltage	48 V input

4.1.2 Actuators

For the active winch, a Robodrive ILM 70x18 motor is combined with a Harmonic Drive CSD-32-2A-160 strain wave gearing, offering a reduction ratio of 1:160 with 60% efficiency. The winch motor delivers 4.05 Nm max. torque, which results in a maximum torque of 388.8 Nm after transmission (Eq. 1). The combined weight of Coyote3 (27.5 kg) and TMDS (23 kg) applies 495.41 Nm of tensile force on the tether (Eq. 2). Hence, the required winch torque of 99.08 Nm can be derived from the spool radius of 0.2 m and the estimated tether force (Eq. 3). Finally, the comparison of τ_{winch} and τ_{req} yields a safety margin of 3.92. The Robodrive ILM 38x12 has a no-load speed of 2120 rpm, which gets reduced to 13.25 rpm after transmission. Therefore, the tether can be reeled with a max. linear velocity of 0.28 m s^{-1} (Eq. 4).

$$\tau_{winch} = \tau_{motor} \cdot \frac{1}{n} \cdot \eta \ , \tag{1}$$

where τ_{winch} = winch torque, τ_{motor} = motor torque, n = gear ratio, η = efficiency.

$$F_T = (m_C + m_T) \cdot g \ , \tag{2}$$

where F_T = tether force, m_C = Coyote3 mass, m_T = TMDS mass, g = 9.81 m s^{-2} .

$$\tau_{req} = F_T \cdot r_s \ , \tag{3}$$

where τ_{req} = required winch torque, r_s = spool radius.

$$v = \omega n \cdot \frac{2\pi r_s}{60} \ , \tag{4}$$

where v = linear velocity, ω = angular velocity in rpm.

The height of the platform can be adjusted by two prismatic joints in order to facilitate docking and transport. The lifting mechanism is actuated by two Robodrive ILM 38x12 motors working in parallel. Each motor provides 0.76 Nm max. torque and is attached to a flanged ball screw nut on a rolled ball screw spindle with 2 mm pitch. Estimating 90% efficiency for rolled ball screw spindles, this gives an axial force of 2148.8 N per spindle (Eq. 5):

$$F_S = \tau_{motor} \cdot \frac{2\pi\eta}{p} \ , \tag{5}$$

where F_S = spindle force, p = pitch.

All three actuators are controlled with a brushless direct current (BLDC) motor driver stack [41]. The BLDC stack contains a motor driver stage as well as a Field Programmable Gate Array (FPGA) and a connection board, allowing local control and telemetry pre-processing, directly within the actuator module.

4.1.3 Interfaces

The device comprises two different space robotic interfaces: On the one hand, a passive EMI at the end of the tether and on the other, a passive HOTDOCK at the topside of the platform. Heavy load tests with the EMI [38] showed that the interface withstands loads up to 400 N acting at angles between 0° and 30°. Furthermore, it can hold a maximum of 1300 N pure tensile force with 0° angle of attack. The androgynous interface supports docking in 90°-steps of orientation. Figure 4 displays how the active EMI at the tip of SherpaTT's manipulator is used to establish a connection with the passive EMI of the TMDS. The 90° symmetrical design of the HOTDOCK allows misalignment of ±15 mm in translation and 10° in rotation, and it has a stated load transfer of 3000 N in traction and 300 Nm in bending moment [39]. Figure 5 depicts how the TMDS is attached to the underbody of Coyote3 with latched active and passive HOTDOCK interfaces.

4.1.4 Communication and Power

In addition to the described hardware interfaces the TMDS features an 2.4 GHz mobile access point, allowing wireless communication between the robotic systems and the TMDS prior to docking. It does not comprise an integrated battery and, thus needs to be powered through one of its interfaces. The input voltage of 48 V is directly used by the three actuators, and a DC/DC converter supplies the other electronic components with 12 V. The power consumption of each component is listed in Table 2. Taking into account the 89% efficiency of the DC/DC converter, 26.3 W are required to power all 12 V components. This adds up to a slightly higher 637, 2 W overall max. power consumption compared to the sum of 634, 3 W shown

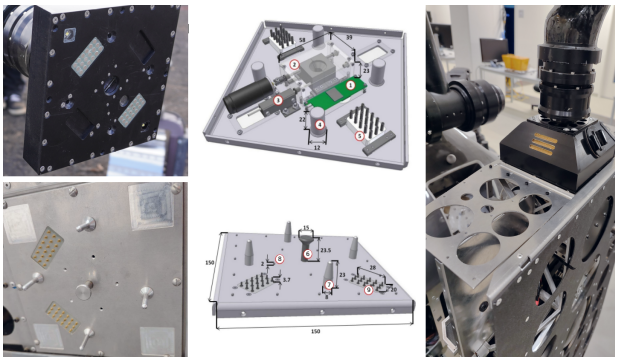

Fig. 4. Active (top left) and passive (bottom left) EMI. CAD design (centre) of the first EMI generation [40] with dimensions in mm: 1) camera, 2) mechanical latch with spindle drive and dust protection housing, 3) linear potentiometer, 4) cylinder with conical mouth, 5) block of contact plates, 6) bolt for latch mechanism, 7) dome-shaped centering pins, 8) distance pins, 9) block of contact probes. SherpaTT's manipulator grasping the TMDS with latched EMI (right).

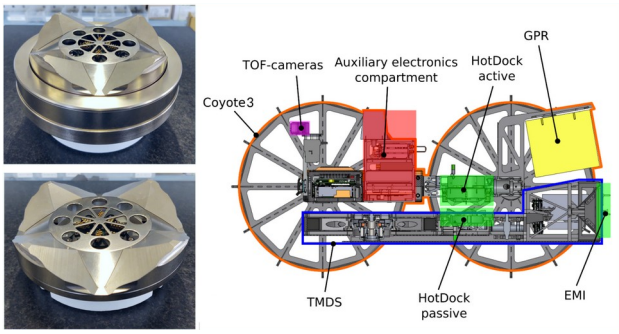

Fig. 5. Active (top left) and passive (bottom left) HOTDOCK interface images from [8]. Sectional view of the TMDS attached to the underbody of Coyote3 with latched HOTDOCK (right).

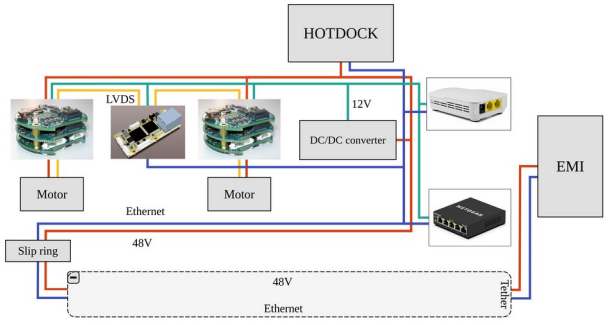

Fig. 6. TMDS simplified circuit diagram.

Table 2. TMDS Power Budget

Part	Voltage [V]	Power [W]	Quantity	total Power [W]
Robodrive ILM 70x18	48	270	1	270
Robodrive ILM 38x12	48	168	2	336
HOTDOCK	48	3.6	1	3.6
EMI	48	1.3	1	1.3
Netgear GS305E	12	2.4	1	2.4
Open-Mesh OM2P	12	10	1	10
BLDC motor driver stack	12	4	2	8
LVDS/Ethernet converter	12	3	1	3
			Sum:	634.3 W

in the power budget. The physical communication layer for low-level actuator control is based on Low-Voltage Differential Signaling (LVDS) and a LVDS to Ethernet converter links low with high-level communication. The protocol used for low-level data exchange is Node-level Data Link Communication (NDLCom) [42]. A simplified circuit diagram of the TMDS is given in Figure 6.

4.1.5 On-board Software

In order to ensure reliable winding and unwinding of the tether, a redundant safety mechanism has been implemented. The low-level safety feature uses register values to specify the minimum and maximum tension directly on the motor stacks FPGA. Only within these bounds would the winch react to incoming commands. On the high-level side, the maximum speed is set to limit incoming commands. The two prismatic joints of the lift mechanism are configured as dependent master and slave joints to keep them synchronized. The master receives the lift command and forwards it to the slave. In this way, mechanical damage is avoided as the joints cannot move independently and will stop with an error state, in case their position diverges over a defined threshold. Since the TMDS has no integrated processing unit for high-level control, all hardware drivers have to run on a robot connected through one of the interfaces. Therefore, Coyote3 and SherpaTT are both running drivers for the lift and winch joints. The drivers run in a pre-operational state and can be started or stopped by the other MP-3 software modules.

4.2 MP-3 Software Modules

4.2.1 TMDS Deployment

At the beginning of MP-3, operators in the Ground Control Station (GCS) identify the most suitable access point for the rappelling operation based on the products from MP-1, a joint map of the surface around the skylight, and MP-2, the full 3D reconstruction of the lava tube entrance. The SherpaTT rover grasps the TMDS, which is initially attached to the body, with its 6 DoF manipulator [43] and deploys it at the selected spot in the vicinity of the skylight (Fig. 7: 1 and 2). After being triggered from the GCS, the *TMDS Deployment* module is executed fully autonomously using an offline-generated manipulator trajectory. The deployment trajectory is described via predefined intermediate

waypoints in the Cartesian space and a motion planner commands a local twist from the current pose of the end-effector to the subsequent pose, once a previous waypoint has been reached. Each state transition waits for the feedback from the trajectory follower that a validation checkpoint has been accomplished before proceeding with the next waypoint. To ensure a smooth deployment in uneven terrain, the rover simultaneously performs multiple tasks. While the manipulator is lowering the TMDS to the ground, the wheeled-legged mobile base is driving backwards using its four 5 DoF legs for active ground adaptation [44], and the tether is synchronously uncoiled. In this way, the full capabilities of the entire 26 DoF redundant floating-based robot are exploited in a compliant multi-contact interaction with the environment. The active EMI at the tip of SherpaTT's manipulator remains connected to the passive EMI at the end of the tether, after the TMDS has been placed on the ground.

4.2.2 Docking Behavior

A camera in the rear axis of Coyote3 is used to detect ArUco [45] markers on the TMDS. When the markers are successfully detected, the pose of the TMDS gets transformed into the robot base frame. Before it is sent to the path planner, it is recalculated with a configurable offset of 1.5 m to receive a goal pose that is at a certain distance in front of the TMDS. The planner generates a trajectory from the current location to the goal pose, and a trajectory follower is used to track it. After Coyote3 has reached the final position and heading, it drives backwards onto the TMDS (Fig. 7: 2 and 3). A mechanical guidance and an end-stop helps to align the passive HOTDOCK interface on the topside of the TMDS with the active counterpart at the underbody of the robot. Coyote3 then uses wireless communication to command the TMDS to raise its upper part. Once the lift mechanism is fully extended (Fig. 7: 4), both HOTDOCK interfaces are in contact and the latch can be closed. Next, the lifting mechanism folds up again, which effectively lifts the TMDS off the ground as it is now firmly attached to the underbody of Coyote3. The *Docking Behavior* is finished and the task stays in the finished state until undocking is externally triggered. In this state, a power and data connection chain between SherpaTT, the TMDS and Coyote3 is established via the tether and through the two space robotic interfaces, EMI and HOTDOCK.

4.2.3 Rappelling Rover Guidance

This software module guides the descent of Coyote3 through the skylight down into the lava tube. It is composed of a descent controller that generates motion commands for Coyote3 and a winch controller to control the release of the tether by the TMDS. *Rappelling Rover Guidance* maps the translational robot

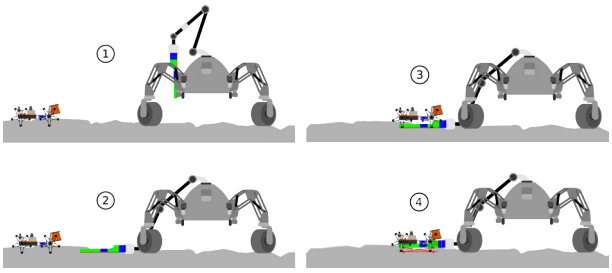

Fig. 7. Initial (1) and final state (2) of the TMDS Deployment as well as intermediate states of the Docking Behavior. Coyote3 is positioned above the TMDS (3) with active and passive HOTDOCK aligned. The lifting mechanism of the TMDS is extended (4), so that the interface can be latched.

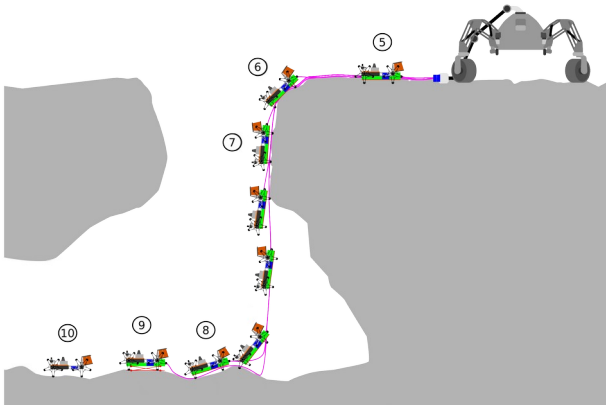

Fig. 8. Rappelling sequence: Coyote3 traversing horizontally (5), on high incline (6) and vertically (7), landing (8), undocking (9) and exploring the lava tube (10).

velocity to a matching angular spooling speed for the winch joint, taking winch radius and gear ratio into account. The descent controller informs the GCS about the rappel progress by estimating the current state of Coyote3 based on IMU and wheel odometry readings.

In a normal descent, Coyote3 goes through four states, shown in Figure 8: traversing horizontally (5), traversing high incline (6), traversing vertically (7) and landing (8). In addition to the nominal sequence, state transitions are included to address the cases of uneven surfaces before reaching the skylight and uneven walls while traversing vertically. Throughout the decent, the tension of the tether needs to be kept in a valid range. A minimum tension on the tether is required to allow the low-level safety mechanism of the winch to unspool, while too much tension would make Coyote3's wheels skid. The winch controller incorporates the rappelling state of Coyote3 and force sensor readings from the TMDS to control the tether tension. This prevents the tether from developing slack, which is crucial to avoid sudden drops of Coyote3 during the vertical descent. As

soon as the landing has been detected and Coyote3 is back in an almost horizontal configuration, the GCS can initiate the undock sequence, where the TMDS lift mechanism extends and the HOTDOCK is unlatched (9). Afterwards the TMDS height is lowered again, and Coyote3 can drive forward to leave the docking station (10).

4.2.4 Mobile Manipulation

Considering the hazard of high torques acting on SherpaTT's manipulator during the rappelling operation, it was necessary to include a controller that aligns the arm's last link and the tether. This alignment ensures the safety of the robotic arm since it eliminates torques from the spherical wrist, which has weaker joints, transferring them to the elbow joints of the manipulator, which are bigger and more resistant. In this regard, the *Mobile Manipulation* component uses optimal control techniques [46] within a Model Predictive Controller (MPC) to react to the tether tension endured by the manipulator, which is measured with a force torque sensor placed in the arm's end-effector. Trying to compensate for these forces and torques, the software module generates new goal poses for the end-effector, which are then followed using MPC. Remark that the mobile manipulation capabilities of SherpaTT give the MPC a lot of possibilities to actively compensate for those efforts, choosing between moving the mobile base, the manipulator, or both at the same time.

All software modules have been developed using the Robot Construction Kit (Rock)[1] and a framework independent interface is provided via a lightweight communication library [47]. This allows to send inter-robot commands from a remote terminal and serves as a debugging interface.

5. Results and Discussion

The primary goal of *TMDS Deployment* was to safely place the TMDS at a designated location near the skylight. The sequence was carried out fully autonomously, and all intermediate states were successfully transmitted to the GCS. The EMI allows a maximum uncertainty in horizontal positioning of ±5 mm and an angular misalignment of 7° between its passive and active counterparts. However, in cases of such misalignments, a sensitive force controller needs to properly align the interfaces during the docking process. Throughout the tests, the readings from the force-torque sensor at the tip of the manipulator were not accurate enough to perform force-based control. As a result, grasping the EMI with the manipulator proved to be challenging. But initial challenges, such as reliably grasping the TMDS, enabling power through the EMI and starting the TMDS joint drivers, were effectively resolved. Diligently calibrating the manipulator and commanding a local twist from the current pose of the end-effector to the subsequent pose were required in order to precisely track all waypoints of the deployment trajectory. In addition, safety checks were added to the implemented state machine, ensuring that the TMDS is fully powered and all drivers have started correctly before proceeding with the next step.

The *Docking Behavior* component was functional in simulation and during the field trials, but Coyote3 was not always able to closely follow the planned trajectory to the goal pose in front of the TMDS. While marker detection, goal transformation, and trajectory planning worked robustly, the robot was unable to track the planned trajectory with sufficient precision. This was mainly due to heading errors as a consequence of faulty odometry through skid drive on the loose terrain in the field. In cases where Coyote3 was manually driven onto the TMDS, the remaining part of the docking sequence was successfully executed without further operator intervention.

Fig. 9. The two rovers, Coyote3 and SherpaTT, with the TMDS during TMDS Deployment (top), Docking Behavior (centre) and start of Rappelling Rover Guidance (bottom).

[1]online: http://www.rock-robotics.org

In cases where Coyote3 was manually driven onto the TMDS, the remaining part of the docking sequence was successfully executed without further operator intervention. In the design process, a certain degree of alignment error was foreseen, and the rounded front in combination with the metal rim, was supposed to provide a passive self-alignment. In some cases, this worked, but in others, the metal grousers of the wheels locked onto the edge of the upper TMDS surface and resulted in Coyote3 running over the TMDS. The undocking procedure worked flawlessly, yet after three weeks of testing in the field, the HOTDOCK was contaminated with dust and particles from the abrasion of volcanic rock. The contamination led to a jammed interface where latching and unlatching was not functional anymore. After disassembling, cleaning and reassembling, the interface worked again. Figure 9 illustrates the initial configuration of MP-3, where the TMDS is attached to the body of ShepaTT, and both robots are positioned close to the skylight. Moreover, the figure displays Coyote3 performing the docking with the TMDS and heading towards the skylight, carrying the TMDS under its chassis while still being connected to the manipulator via the tether.

Given the amount of information gathered about the skylight in MP-1 and MP-2, the rappelling was expected to be rather simple in terms of guidance. Nevertheless, the communication delay between the Moon and Earth requires some level of autonomy, especially if fast reaction times are needed to compensate for possible unpredicted events.

The main purpose of *Rappelling Rover Guidance* was to maintain a stable tension on the tether during the descent of Coyote3 and to control the wheel motions. During the first test, it was identified that the tension on the tether after landing was too large, which led to pulling up the back of the TMDS and thus making it difficult for the robot to undock from the TMDS. For that reason, an additional release of tether without any wheel motion was introduced in this last stage of the descent. The mission phase lasted a total of 8 minutes, during which Coyote3 was abseiling for around 2 min to descend 5 meters at an average speed of 0.05 m s^{-1} until it reached the bottom of the lava tube. The touchdown was correctly recognized by the software component based on the pitch of the robot. Figure 10 shows images from the field tests where Coyote3 enters the skylight, rappels down the vertical walls, reaches the bottom of the lava tube, undocks from the TMDS, and begins to explore the lava tube system.

The *Mobile Manipulation* module actively compensated forces and torques that the tether applied to SherpaTT's manipulator. The manipulator reacted compliantly to the tether tension. It became more flexible when high tensile forces occurred and moved back to a predefined pose whenever the forces acting on it decreased. As a result, the maximum peak torque endured by the wrist joints during the rappel was 25.12 Nm with an average of 4.08 Nm, which is far lower than their maximum tolerable torque (92 Nm).

Lastly, the TMDS demonstrated its robustness in all stages of MP-3 by ensuring a firm connection with Coyote3 through the HOTDOCK interface and by unwinding the tether at the desired velocity without entanglements in the spool. It provided power and data transmission while docked, but also served as a wireless communication relay between the rover in the lava tube and the rover at the skylight entrance during the subsequent exploration phase.

5. Conclusions

The TMDS underwent rigorous testing and refinement, leading to significant advancements and successful outcomes. Coyote3 was able to safely reach the bottom of the lava tube in multiple tests during the field trials. In the following, we share valuable findings from the extensive tests by listing benefits and shortcomings of the newly developed hardware:

- A main limitation for existing TRs is the length of the tether, which imposes a hard constraint on the area that can be explored. For this reason, the developed TMDS allows a scout rover to attach and detach to get energy, communicate with the GCS or to explore the surroundings.
- After detaching, the tether does not have to be further considered by the navigation algorithm, hence the risk of entanglement with the tether is reduced during subsurface exploration.
- The TMDS features two standard space interconnects, enabling any rover with the corresponding counterparts to participate in a rappelling operation. However, it must be thoroughly evaluated whether the interfaces meet the specific requirements of the mission in terms of dust resistance, mechanical strength, tolerance of misalignment, power and data transmission rates.
- A commercial submarine tether was used here, but the tether should be carefully selected in a real planetary mission. A sheath with high abrasive resistance must provide protection against sharp-edged lava rocks, while weight and elasticity are other important properties.
- In an updated version of the TMDS, we would revise the mechanical guidance on the TMDS in conjunction with the underbody of the scout rover to guarantee a reliable docking behavior under non-ideal conditions.

- Another drawback of the presented approach is the requirement for a rather flat ground in the deployment area near the skylight and in the touch-down zone at the bottom of the lava tube. None of the areas should be covered with large boulders, which would prevent smooth docking and undocking operations. Fortunately, detailed photographs of the planetary surface are likely available in a real space mission in advance from an orbiter.

In summary, this work presents a solution to access lunar lava tubes with a heterogeneous team of rovers, and the TMDS plays a key role in achieving the objectives of the Lunar Analogue Mission. The results demonstrate the feasibility of the outlined multi-robot rappelling scenario and confirm the effectiveness of the developed system.

Lava tubes and other cavities on the Moon and Mars are of high scientific interest, and there is great opportunity that in the near future a multi-robot team will be able to explore them.

Acknowledgments

The presented work was funded by the European Union's Horizon 2020 research and innovation programme – Operational Grant No. 101004130 and the dissemination was supported by the Federal Ministry for Economic Affairs and Climate Action – Operational Grant No. 68GX21003H. The authors would like to thank the CoRob-X team for the good and successful collaboration within the project.

Fig. 10. Coyote3 starts the descent through the skylight (1), rappels down the vertical walls (2), reaches the bottom of the lava tube (3), undocks from the TMDS (4) and begins the subsurface lava tube exploration (5-6).

References

[1] Arancón M M et al. 2017 ESROCOS: A Robotic Operating System for Space and Terrestrial Applications, In Proceedings of the 14th Symposium on Advanced Space Technologies in Robotics and Automation, ESA-ESTEC (Noordwijk, the Netherlands)

[2] Ocón J et al. 2017 ERGO: a Framework for the Development of Autonomous Robots, In Proceedings of the 14th Symposium on Advanced Space Technologies in Robotics and Automation, ESA-ESTEC (Noordwijk, the Netherlands)

[3] Dominguez R, Post M, Fabisch A, Michalec R, Bissonnette V and Govindaraj S 2020 International Journal of Advanced Robotic Systems 17 pp. 1-15

[4] Dubanchet V and Andiappane S 2018 Development of I3DS: An Integrated Sensors Suite for Orbital Rendezvous and Planetary Exploration, In Proceedings of the 14th International Symposium on Artificial Intelligence, Robotics and Automation In Space (Madrid, Spain)

[5] Vinals J et al. 2018 Future Space Missions With Reconfigruable Modular Payload Modules And Standard Interface – An Overview Of The SIROM Project, In Proceedings of the 69th International Astronautical Congress (Bremen, Germany)

[6] Suatoni M et al. 2018 FACILITATORS – Facilities for testing orbital and surface robotics building blocks, In Proceedings of the 69th International Astronautical Congress (Bremen, Germany)

[7] Dubanchet V et al. 2021 EROSS project – Ground validation of an autonomous GNC architecture towards future European servicing missions, In Proceedings of the 72nd International Astronautical Congress (Dubai, United Arab Emirates)

[8] Roa G M A et al. 2022 PULSAR: Testing the Technologies for In-Orbit Assembly of a Large Telescope, In Proceedings of the 16th Symposium on Advanced Space Technologies in Robotics and Automation, ESA-ESTEC (Noordwijk, the Netherlands)

[9] Letier P et al. 2019 MOSAR: Modular Spacecraft Assembly and Reconfiguration Demonstrator, In Proceedings of the 15th Symposium on Advanced Space Technologies in Robotics and Automation, ESA-ESTEC (Noordwijk, the Netherlands)

[10] Ocón J et al. 2020 ADE: Autonomous Decision Making in Very Long Traverses, In Proceedings of the 15th International Symposium on Artifical Intelligence, Robotics and Automation in Space (Virtual Conference)

[11] Govindaraj S et al. 2019 PRO-ACT: Planetary Robots Deployed For Assembly And Construction of Future Lunar ISRU and Supporting Infrastructure, In Proceedings of the 15th Symposium on Advanced Space Technologies in Robotics and Automation, ESA-ESTEC (Noordwijk, the Netherlands)

[12] Estable S et al. 2023 J. Phys.: Conf. Ser. 2526 012121

[13] Dettmann A et al. 2022 CoRoB-X: A Cooperative Robot Team for the Exploration of Lunar Skylights, In Proceedings of the 16th Symposium on Advanced Space Technologies in Robotics and Automation, ESA-ESTEC (Noordwijk, the Netherlands)

[14] Vögele T et al. 2023 CoRoB-X: Demonstration of A Cooperative Robot Team in Extensive Field Tests, In Proceedings of the 17th Symposium on Advanced Space Technologies in Robotics and Automation, ESA (Scheltema, Leiden, the Netherlands)

[15] Daga A, Allen C, Battler M, Burke J D, Crawford I, Léveillé R, Simon S, and Tan L T 2009 Lunar and martian lava tube exploration as part of an overall scientific survey (LPI Contributions)

[16] Oberbeck V R et al. 1969 Mod. Geol.1 pp.75-80

[17] Léveille R J and Datta S Planetary and Space Science 58 pp. 592-98

[18] Arya A, Rajasekhar R, Thangjam G, Ajai and Kumar A S K 2011 Current science 100 4 pp. 524-29

[19] Sonsalla R U et al. 2022 Towards a Semi-Autonomous Robotic Exploration of a Lunar Skylight Cavity, In Proceedings of the 43rd IEEE Aerospace Conference (Big Sky, MT, USA) pp. 1-20

[20] Dominguez R et al. 2023 Field Testing of Cooperative Multi-Robot Technology for Accessing and Exploring a Planetary Lava Tube, In Proceedings of the 4th International Planetary Caves Conference (Haría, Lanzarote),

[21] Cordes F and Babu A 2016 A Versatile Hybrid Wheeled-Leg Rover, In Proceedings of the 13th International Symposium on Artificial Intelligence, Robotics and Automation In Space (Beijing, China)

[22] Sonsalla R, Bessekon J and Kirchner F 2015 CoyoteIII: Development of a Modular and highly Mobile Micro Rover, In Proceedings of the 13th Symposium on Advanced Space Technologies in Robotics and Automation, ESA-ESTEC (Noordwijk, the Netherlands)

[23] Gancent J et al. 2021 LUVMI-X: An Innovative Instrument Suit and Versatile Mobility Solution for Lunar Exploration, In Proceedings of the 72nd International Astronautical Congress (Dubai, United Arab Emirates)

[24] Ciarletti V et al. 2017 Astrobiology 17(6-7) (New York: Mary Ann Liebert, Inc.) pp. 565–84

[25] Van Winnendael M, Baglioni P, Vago J 2005 Development of the ESA ExoMars Rover, In Proceedings of the 8th International Symposium on Artifical Intelligence, Robotics and Automation in Space (Munich, Germany)

[26] Chen Y, Huang R, Ren X, He L and He Y 2013 ISRN Astronomy and Astrophysics 2013 3711
[27] Steltzner A et al. 2006 Mars Science Laboratory entry, descent, and landing system, In Proceedings of the 2006 IEEE Aerospace Conference (Big Sky, MT, USA) 9 pp. 15
[28] Wettergreen D, Thorpe C and Whittaker R 1993 Robotics and Autonomous Systems 11 3 pp. 171-85
[29] Huntsberger T, Stroupe A W, Aghazarian H, Garrett M, Younse P und Powell M 2007 J. Field Robotics 24 64 pp. 1015–31
[30] McGarey P, Pomerleau F und Barfoot T 2015 System Design of a Tethered Robotic Explorer (TReX) for 3D Mapping of Steep Terrain and Harsh Environments, In Proceedings of the 10th International Symposium on Field and Service Robotics (Toronto, Canada)
[31] McGarey P, Yoon D, Tang T, François Pomerleau F and Barfoot T D 2017 J. Field Robotics 35 8 pp. 1327-41
[32] Nesnas I et al. 2012 J. Field Robotics 29 4 pp. 663-85
[33] Bartsch S 2013 Development, Control, and Empirical Evaluation of the Six-Legged Robot SpaceClimber Designed for Extraterrestrial Crater Exploration (University of Bremen, Germany)
[34] McGarey P, Nguyen T, Pailevanian T and Nensas I A 2020 Design and test of an electromechanical rover tether for the exploration of vertical lunar pits, In Proceedings of the 41st IEEE Aerospace Conference (Big Sky, MT, USA) pp. 1-10
[35] Nesnas I et al. 2023 Acta Astronautica 211 pp. 163-176
[36] Yan X, Brinkmann W, Palazzetti R, Melville C, Li Y, Bartsch S and Kirchner F 2018 Frontiers in Robotics and AI 5 64
[37] Vinals J, Gala J and Guerra G 2020 Standard Interface for Robotic Manipulation (SIROM): SRC H2020 OG5 Final Results - Future Upgrades and Applications, In Proceedings of the 15th International Symposium on Artifical Intelligence, Robotics and Automation in Space (Virtual Conference)
[38] Brinkmann W, Cordes F and Kirchner F 2015 A Robust Electro-Mechanical Interface for Cooperating Heterogeneous Multi-Robot Teams, In Proceedings of the International Conference on Intelligent Robots and Systems IEEE/RSJ (Hamburg, Germany)
[39] Letier P et al. 2020 HOTDOCK: Design and Validation of a New Generation of Standard Robotic Interface for On-Orbit Servicing, In Proceedings of the 71st International Astronautical Congress (Virtual Conference)
40] Dettmann A, Zhuowei W, Brinkmann W, Cordes F and Kirchner F 2011 Heterogeneous Modules with a Homogeneous Electromechanical Interface in Multi-Module Systems for Space Exploration, In Proceedings of the IEEE International Conference on Robotics and Automation (Shanghai, China)
[41] Hilljegerdes J, Kampmann P, Bosse S and Kirchner F 2009 Development of an Intelligent Joint Actuator Prototype for Climbing and Walking Robots, In Proceedings of the 12th International Conference on Climbing and Walking Robots and the Support Technologies for Mobile Machines (Istanbul, Turkey)
[42] Zenzes M, Kampmann P, Schilling M and Tobias S 2016 NDLCom: Simple Protocol for Heterogeneous Embedded Communication Networks, In Proceedings of the 14th Embedded World Exhibition and Conference (Nürnberg, Germany)
[43] Manz M, Hilljegerdes J, Dettmann A and Kirchner F 2012 Development of a Lightweight Manipulator Arm using Heterogeneous Materials and Manufacturing Technologies, In Proceedings of the 11th International Symposium on Artifical Intelligence, Robotics and Automation in Space (Turin, Italy)
[44] Cordes F, Ajish B and Kirchner F 2017 Static force distribution and orientation control for a rover with an actively articulated suspension system, In Proceedings of the IEEE/RSJ International Conference on Intelligent Robots and Systems (Vancouver, Canada) pp. 5219-24
[45] Garrido-Jurado S, Muñoz-Salinas R, Madrid-Cuevas F J and Marın-Jiménez M J 2014 Pattern Recognition 47 6 (Amsterdam: Elsevier) pp. 2280-92
[46] Paz-Delgado G J, Pérez-del-Pulgar C J, Azkarate M, Kirchner F and García-Cerezo A 2023 Intelligent Service Robotics 16 pp. 247–63
[47] Danter, L et al. 2020 Lightweight and Framework-Independent Communication Library to Support Cross-Platform Robotic Applications and High-Latency Connections, In Proceedings of the 15th International Symposium on Artificial Intelligence, Robotics and Automation in Space (Virtual Conference)